3002 *Chem. Mater.* **2009,** *21,* 3002–3007
DOI:10.1021/cm900693r

CHEMISTRY OF MATERIALS
Article

$BaTiO_3$, $SrTiO_3$, $CaTiO_3$, and $Ba_xSr_{1-x}TiO_3$ Particles: A General Approach for Monodisperse Colloidal Perovskites

Ahmet Faik Demirörs* and Arnout Imhof*

Soft Condensed Matter, Debye Institute for Nanomaterials Science, Department of Physics and Astronomy, Utrecht University, Princetonplein 5, 3584 CC Utrecht, The Netherlands

Received March 11, 2009. Revised Manuscript Received April 27, 2009

We describe a novel general method for synthesizing monodisperse colloidal perovskite particles at room temperature by postsynthesis addition of metal hydroxides to amorphous titania colloids. In previous work, we used titania particles to synthesize homogenously mixed silica−titania composite particles by addition of a silica precursor to the titania particles (Demirörs et al. Chem. Mater., 2009, *21*, 979). Here we show that the principle is general and can be used to prepare different titania-based composite beads. We demonstrate the synthesis of colloidal perovskites like $BaTiO_3$, $SrTiO_3$, $CaTiO_3$ and $Ba_{0.5}Sr_{0.5}TiO_3$, which have importance for the electronics industry for their dielectric properties. Mixed perovskites like $Ba_xSr_{1-x}TiO_3$ bring tunability in structure and properties by changing the ratio of metal cations. We also show fabrication of metal core, $BaTiO_3$ shell particles, which could find applications in percolative capacitors, and luminescence properties of Pr^{3+} doped colloidal perovskites.

1. Introduction

The fabrication of perovskites (oxides with the formula ABO_3) is of great scientific and technological interest for their ferroelectric, pyroelectric, piezoelectric, dielectric, and catalytic properties.[1−3] Barium titanate, one of the most investigated perovskite materials, has a high dielectric constant[4−6] and ferroelectric properties[7,8] that are essential for thin-film electronic components and electro-optical materials.[3,9−12] It is heavily used in industry as dielectric material component of class II ceramic capacitors.[13] $BaTiO_3$ exists in various crystallographic structures, of which the tetragonal and cubic polymorphs are the most studied. Although the tetragonal polymorph is the thermodynamically stable form at room temperature, most synthesis routes result in the cubic structure, and a high temperature treatment at around 1100 °C is necessary to induce phase transformation from the cubic to the tetragonal structure, which persists upon cooling again to room temperature.[5,6,14]

The tetragonal polymorph of $BaTiO_3$ is ferroelectric and the cubic polymorph is paraelectric. Crystallographic structures determine the dielectric properties, and one way of changing the structure is making mixed perovskites. It is well established that the Fermi level and polymorph stable at room temperature can be tuned by making mixed perovskite structures.[15,16] For $SrTiO_3$, the thermodynamically stable form at room temperature is cubic, and for $CaTiO_3$, it is orthorhombic.[17] $SrTiO_3$ has often been used as a dielectric and photoelectric material, whereas $CaTiO_3$ is recently getting attention for its biocompatibility and implant bone applications[18,19] besides its use in electronics.[20]

Reports for the preparation of micrometer-sized colloidal perovskites are mostly based on hydrothermal treatment of amorphous titania particles with metal salts.[21,22]

*Corresponding authors: A.F. Demirörs, a.f.demirors@uu.nl, Tel: +31 30 253 2315, Fax: +31 30 253 2706; A. Imhof, E-mail: a.imhof@uu.nl, Tel: +31 30 253 2423, fax +31 30 253 2706; www.colloid.nl.

(1) Chandler, C. D.; Roger, C.; Hampden-Smith, M. J. *Chem. Rev.* **1993**, *93*, 1205–1241.
(2) Pena, M. A.; Fierro, J. L. G. *Chem. Rev.* **2001**, *101*, 1981–2017.
(3) Bhalla, A. S.; Guo, R.; Roy, R. *Mater. Res. Innovations* **2000**, *4*, 3–26.
(4) Dutta, P. K.; Asiaie, R.; Akbar, S. A.; Zhu, W. D. *Chem. Mater.* **1994**, *6*, 1542–1548.
(5) Her, Y.-S.; Matijevic, E.; Chon, M. C. *J. Mater. Res.* **1995**, *10*, 3106–3114.
(6) Takeuchi, T.; Tabuchi, M.; Ado, K.; Honjo, K.; Nakamura, O.; Kageyama, H.; Suyama, Y.; Ohtori, N.; Nagasawa, M. *J. Mater. Sci.* **1997**, *32*, 4053–4060.
(7) Lee, T.; Aksay, I. A. *Cryst. Growth Des.* **2001**, *1*, 401–419.
(8) Chen, Z. X.; Chen, Y.; Jiang, Y. S. *J. Phys. Chem. B* **2001**, *105*, 5766–5771.
(9) Setter, N.; Waser, R. *Acta Mater.* **2000**, *48*, 151–178.
(10) Hennings, D.; Klee, M.; Waser, R. *Adv. Mater.* **1991**, *3*, 334–340.
(11) Haertling, G. H. *J. Am. Ceram. Soc.* **1999**, *82*, 797–818.
(12) Lee, J.-Y.; Lee, J.-H.; Hong, S.-H.; Lee, Y. K.; Choi, J.-Y. *Adv. Mater.* **2003**, *15*, 1655–1658.
(13) Moreno, J.; Dominguez, J. M.; Montoya, A.; Vicente, L.; Viveros, T. *J. Mater. Chem.* **1995**, *5*, 509.
(14) Clark, I. J.; Takeuchi, T.; Ohtori, N.; Sinclair, D. C. *J. Mater. Chem.* **1999**, *9*, 83–91.
(15) Kyomen, T; Sakamoto, R.; Sakamoto, N.; Kunugi, S.; Itoh, M. *Chem. Mater.* **2005**, *17*, 3200–3204.
(16) Qin, S.; Becerro, A. I.; Seifert, F.; Gottsmanna, J.; Jiang, J. *J. Mater. Chem.* **2000**, *10*, 1609–1615.
(17) McQuarrie, M. *J. Am. Ceram. Soc.* **1955**, *38*, 444.
(18) Pecharromon, C.; Esteban-Betegon, F.; Bartolome, J. F.; Lopez-Esteban, S.; Moya, J. S. *Adv. Mater.* **2001**, *13*(20), 1541.
(19) Ohtsu, N.; Sato, K.; Yanagawa, A.; Saito, K.; Imai, Y.; Kohgo, T.; Yokoyama, A.; Asami, K.; Hanawa, T. *J. Biomed. Mater. Res. A* **2007**, *82A*(2), 304.
(20) Lemanov, V. V.; Sotnikov, A. V.; Smirnova, E. P.; Weihnacht, M.; Kunze, R. *Solid State Commun.* **1999**, *110*, 611–614.
(21) Wang, Y.; Xu, H.; Wang, X.; Zhang, X.; Jia, H.; Zhang, L.; Qiu, J. *J. Phys. Chem. B* **2006**, *110*, 13835–13840.
(22) Choi, J. Y.; Kim, C. H.; Kim, D. K. *J. Am. Ceram. Soc.* **1998**, *81*(5), 1353–1356.

Published on Web 05/14/2009

However these particles usually are composed of nanosized smaller primary particulates, and upon sonication, the particles readily disintegrate, which is basically an outcome of the harsh conditions of the hydrothermal treatment. Recently Niederberger et al.[23] and O'Brien et al.[24] succeeded in synthesizing monodisperse and highly crystalline $BaTiO_3$ particles in organic media; however these particles are on the order of 5−10 nm. One notable method for nanometer-sized perovskites was the inverse micellar synthesis of Su et al.,[25] which decreased the synthesis temperature to as low as 80 °C. An epitaxial self-assembly method was used by Calderone et al.[26] to synthesize submicrometer-sized $SrTiO_3$ cubical and spherical particles, but this work was not applicable to all metal salts but to only Sr.

Here we present a new method based on a mild post-synthesis treatment to amorphous and porous titania particles. It yields monodisperse colloidal perovskites that are strong enough to withstand sonication and can thus be easily redispersed. Compared with the conventional method used in industry, which is based on solid−solid reaction of the barium salt (usually $BaCO_3$) with anatase titania at elevated temperatures, our method is advantageous in bringing the barium and titanium into nanometer level contact, which decreases the time and the cost for the crystal formation. Especially for the industrial production where monodispersity and size is usually not the most crucial priority, the synthesis of titania can be done in a rougher way in the presence of a polymer surfactant, which we think will have similar properties (porosity, particle size, etc.) to our titania beads. Additionally our method is facile for its availability for post-synthesis intervention like adding different types of metal salts with different ratios, which opens a way to tune the structure and the dielectric properties or to dope the structure with rare earth metals for luminescence.

2. Experimental Section

The synthesis of colloidal perovskite particles is based on the conversion of titania particles. We synthesized the titania particles according to the procedure of Eiden-Assmann et al.[27] with slight modifications. In a typical synthesis, 250 mL of ethanol with 17.0 mL of $Ti(OC_2H_5)_4$ was mixed with 750 mL of ethanol with 4.0 mL of 0.1 M aqueous Lutensol ON50 (BASF) solution. This gave monodisperse titania particles with a size between 900 and 1200 nm depending on the reaction temperature and the amount of the titania precursor. The titania particles collected by centrifugation were then dispersed in fresh ethanol without drying. For confocal microscopy measurements, fluorescent rhodamine isothiocyanate (RITC) dye was added to the dispersion of the particles, and the particles were collected by centrifugation afterward. Because the dye was only physisorbed to the particles, the particles were not washed more then twice. Perovskites with the general formula $ATiO_3$ (where A = Ba, Sr, Ca, or a mixture of Ba and Sr.) were achieved by adding 1:1 A/Ti mole ratio of $A(OH)_2$ salt into the ethanolic dispersion of titania particles. In a typical preparation, for 0.035 g of titania beads dispersed in 10 mL of ethanol, we have added 0.046 g of $Sr(OH)_2$, 0.064 g of $Ba(OH)_2$, or 0.021 g of $Ca(OH)_2$. The mixed dispersions were sonicated for 20−30 min and collected by centrifugation, then dried in a 50 °C oven, which resulted in perovskite gels. The perovskite particles form also without a sonication step, but the sonication step improved contact between the insoluble metal salt and the particles. Perovskite gels were calcined at various temperatures between 700 and 1200 °C for 1 h to obtain crystalline perovskites. Particles were redispersed in ethanol by sonication.

$Ag@BaTiO_3$ particles were synthesized from $Ag@TiO_2$ core−shell particles with an amorphous titania shell. $Ba(OH)_2$ salt was added to $Ag@TiO_2$ particles dispersed in ethanol with 1:1 Ba/Ti mole ratio, and a similar route to perovskites was followed. The Ag particles were prepared using the method of Tao et al.[28] and coated in a similar way to the synthesis of titania particles by using Lutensol ON 50 surfactant.

The powder X-ray diffraction (XRD) measurements were performed with a Philips PW 1820 difractometer with a Philips PW 1729 X-ray generator (Cu Kα radiation). We used either a glass or an aluminum substrate for the XRD measurements.

Transmission electron microscopy (TEM) images were obtained with a Philips Tecnai 12 transmission electron microscope with an accelerating voltage of 120 keV. Samples for TEM were prepared by dipping copper 300 mesh carrier grids covered with carbon-coated Formvar films into dilute suspensions.

Scanning electron microscopy (SEM) micrographs were obtained with a Philips XL 30 FEG scanning electron microscope, and the samples were prepared by drying a drop of particle suspension on a SEM stub.

The fluorescently labeled particles were imaged using an inverted Leica confocal scanning laser microscope (CSLM), type TCS-SP2. The microscope was operated in the fluorescence mode. The 543 nm line of a green He−Ne laser was used for excitation of the rhodamine-labeled particles.

Luminescence spectra were obtained with a Perkin-Elmer LS 50B luminescence spectrometer.

3. Results and Discussion

In our previous work, we have found that amorphous titania particles are very sensitive to drying; particles dried in oven at 50 °C for 2 h could be coated with silica under Stöber conditions, which yielded core−shell particles.[29] However, particles treated with silica prior to drying formed homogenously mixed composite TiO_2−SiO_2 particles.[30] The formation of homogeneously mixed composite particles proves that particles as-synthesized are porous and open to the access of the species added after the synthesis. The porosity difference between dried and nondried particles could also be observed by addition

(23) Niederberger, M.; Bartl, M. H.; Stucky, G. D. *J. Am. Chem. Soc.* **2004**, *126*, 9120–9126.
(24) O'Brien, S.; Louis, B.; Murray, C. B. *J. Am. Chem. Soc.* **2001**, *123*, 12085–12086.
(25) Su, K.; Nuraje, N.; Yang, N. L. *Langmuir* **2007**, *23*, 11369–11372.
(26) Calderone, V. R.; Testino, A.; Buscaglia, M. T.; Bassoli, M.; Bottino, C.; Viviani, M.; Buscaglia, V.; Nanni, P. *Chem. Mater.* **2006**, *18*, 1627–1633.
(27) Eiden-Assmann, S.; Widoniak, J.; Maret, G. *Chem. Mater.* **2004**, *16*, 6.
(28) Tao, A.; Sinsermsuksakul, P.; Yang, P. *Angew. Chem., Int. Ed.* **2006**, *45*, 4597.
(29) Stöber, W.; Fink, A.; Bohn, E. *J. Colloid Interface Sci.* **1968**, *26*, 62.
(30) Demirörs, A. F.; van Blaaderen, A.; Imhof, A. *Chem. Mater.* **2009**, *21*, 979.

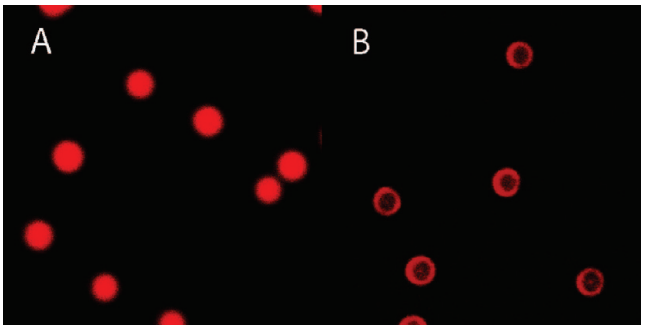

Figure 1. Confocal microscopy image of (A) as-synthesized titania particles after addition of fluorescent dye and (B) dried titania particles after addition of fluorescent dye. Dye adsorbs only on the surface of dried particles. It should be noted that the point spread function of the confocal microscope has a width of 250 nm, close to the width of the rings in panel b. (Image size of panel a = 8.38 μm × 8.38 μm and of panel b = 14.68 μm × 14.68 μm).

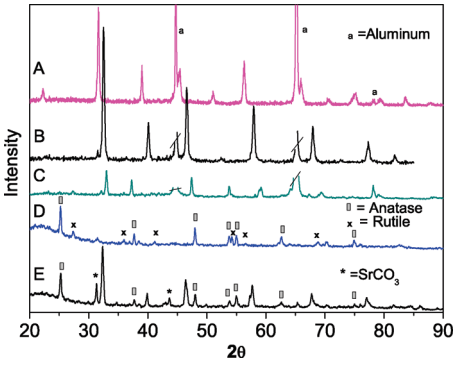

Figure 2. XRD patterns of colloidal perovskites (A) $BaTiO_3$ calcined at 900 °C, (B) $SrTiO_3$ calcined at 850 °C, and (C) $CaTiO_3$ calcined at 1000 °C and of (D) core−shell $BaTiO_3$ and (E) core−shell $SrTiO_3$ particles synthesized by mixing Ba and Sr salts with dried titania particles, which include anatase, rutile, and perovskite peaks also. The peaks at 44.7° and 65.3° and 78.2° at in panels A, B, and C are due to the aluminum substrate and the broad peak around 25° in panels D and E belongs to the glass substrate. The aluminum lines are cut in (b) and (c).

of a fluorescent dye (RITC) to dispersions of either type of particle (Figure 1). Although the dye molecules could reach the inner parts of the as-synthesized particles yielding fully dyed particles (Figure 1A), dried particles fluoresced only on the surface, indicating that the dye could adsorb on the outer surface of the particle but no further (Figure 1B).

In this article, we demonstrate that this principle for making composite particles by postsynthesis addition of new components is general and can be applied to make perovskite gels by adding metal salts with 1:1 A/Ti mole ratio to the titania particles. Sonication improves nanometer level contact between metal oxides and highly porous titania. A better contact between species stimulates the formation of crystalline perovskite structures upon calcination at 700−900 °C. Figure 2A,B,C shows the XRD patterns of the colloidal $BaTiO_3$, $SrTiO_3$, and $CaTiO_3$ powders synthesized. The XRD patterns only include the peaks of the pure perovskite structures and have no peaks of impurities like $BaCO_3$ or $SrCO_3$ nor peaks of anatase or rutile titania. Since no washing steps were used for the XRD measurements, this indicates that perovskite gel formation is close to stoichiometric and no impurities exist. These XRD patterns can be indexed to cubic $BaTiO_3$ (JCPDS No. 74-1968), $SrTiO_3$ (JCPDS No. 73-0661), and $CaTiO_3$ (JCPDS No. 22-153). To demonstrate the fact that the perovskite gel formation only occurs stoichiometrically if the titania is not dried, we added 1:1 A/Ti ratio metal salts to the dried particles and calcined the sonicated mixture. The resulting XRD patterns are given in Figure 2D,E and show clear peaks of anatase, rutile, and $SrCO_3$ impurities. This proves that drying prevents pore access of added species so that titania particles after calcination become anatase or a mix of anatase and rutile, whereas the excess Sr salt forms $SrCO_3$ by capturing CO_2 from air or stays as amorphous BaO in case of Ba salt. In Figure 2D, the (101) peak of $BaTiO_3$ is barely visible, whereas in Figure 2E the $SrTiO_3$ titanate peaks are more pronounced. Perovskite formation is not complete for dried particles and leaves some nonreacted free titania and metal salt, which upon calcination forms anatase, rutile, or carbonate impurities.

SEM images (Figure 3) show that the perovskite particles are well-defined spheres. However it is also observed that the surface is very rough, which indicates that the particles are porous. Crystalline domains were visible from the HR-SEM images with domain sizes in the range 70−100 nm for $BaTiO_3$; the domain sizes were smaller in $SrTiO_3$, ranging from 20 to 60 nm, and intermediate for the $Ba_{0.5}Sr_{0.5}TiO_3$ with 50−70 nm domain size. The larger domain sizes for $BaTiO_3$ caused a structure with macropores inside, whereas particle surfaces were smoother in $SrTiO_3$ particles, and the surface roughness was in between for the $Ba_{0.5}Sr_{0.5}TiO_3$. It should also be noted that these perovskite particles had a size of 1.5 μm whereas the initial amorphous titania particles were only 1.2 μm after drying. This difference was caused by the incorporation of the metal salts in the structure. The titania particles (in a solvent) prior to drying were much larger in size, and upon drying, particles shrank and densified. In our previous work, we have found that amorphous titania particles prior to drying were as large as 1.8 μm and shrank to 1.3 μm upon drying, determined by the static light scattering technique.[30] This result shows that there is enormous shrinkage of the as-synthesized particles after drying. However addition of the metal salts fills the pores and lowers the amount of shrinkage to 1.5 μm in the fabrication of perovskites.

The microstructure of the particles was also investigated by means of TEM. Figure 4A,B,C shows the TEM images of $BaTiO_3$, $SrTiO_3$, and $Ba_{0.5}Sr_{0.5}TiO_3$, respectively. The sphericity of the titania particles was preserved during the synthesis of perovskites. It can be concluded from these images that the particles are monodisperse and do not disintegrate upon sonication. From image analysis of TEM and SEM pictures, we have found the size and polydispersity of $BaTiO_3$, $SrTiO_3$, and $Ba_{0.5}Sr_{0.5}TiO_3$ particles to be 1.5 μm with 5% polydispersity, 1.6 μm with 10% polydispersity, and 1.4 μm with 5% polydispersity, respectively. The polydispersity of the final particles is determined by the polydispersity of the initial titania particles, and these values agree with our findings

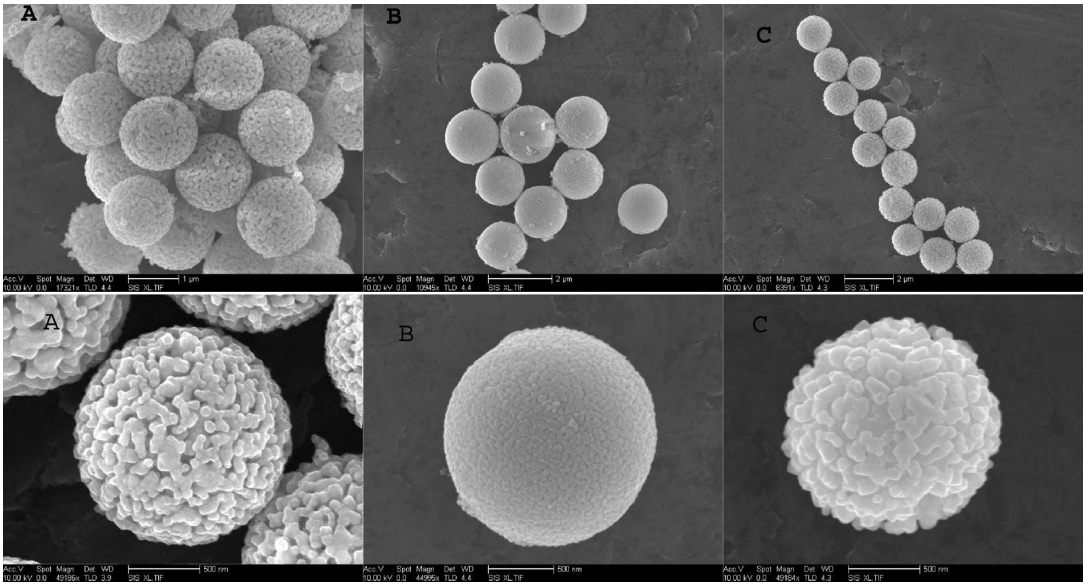

Figure 3. SEM images of the (A) $BaTiO_3$ particles calcined at 900 °C, (B) $SrTiO_3$ particles calcined at 850 °C, and (C) $Ba_{0.5}Sr_{0.5}TiO_3$ particles calcined at 900 °C. The images below are magnified HR-SEM images for better visibility of the porous structure.

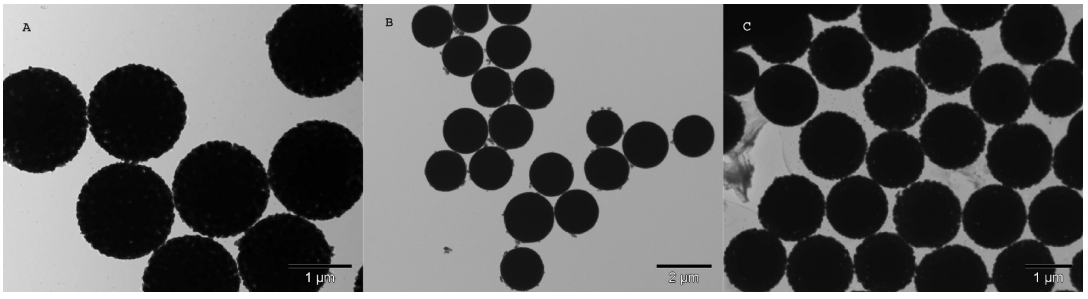

Figure 4. TEM images of (A) $BaTiO_3$ particles calcined at 900 °C, (B) $SrTiO_3$ particles calcined at 850 °C, and (C) $Ba_{0.5}Sr_{0.5}TiO_3$ particles calcined at 900 °C. All particles were sonicated several minutes prior to deposition on a TEM grid.

for the titania particle polydispersities in the earlier work.[30] EDX spectra made on a point on the perovskite particles showed both Ti and metal peaks (Supporting Information, Figure S1A,B). The Ba and Ti peaks are closely spaced and partially overlapping, so we made an energy-dispersive X-ray (EDX) profile on a single particle for the $SrTiO_3$, which showed that Sr was homogeneously spread inside the particle (Supporting Information, Figure S1C,D). The EDX line profiles on $SrTiO_3$ particles were made for particles both before and after calcination to show that the metal cations were spread through the particle already prior to the calcination step. EDX line profiles for gel and crystalline $SrTiO_3$ particles are identical, which shows that metal cations are spread through the particle after the sonication step. The easy formation of the perovskite gels just after sonication actually explains how crystalline perovskite can be formed by only a short calcination.

The $BaTiO_3$ particles after calcination at 700−900 °C had the cubic lattice, which is known to be paraelectric. Phase transformation from the cubic to the ferroelectric tetragonal polymorph of $BaTiO_3$, which is the stable form at room temperature, can be induced by calcining the cubic sample to 1100−1300 °C. We calcined our $BaTiO_3$ particles at 1200°C to observe the phase transformation from cubic to tetragonal. In the literature, the phase transformation is usually detected from the splitting of the (200) peak cubic at 45.4° into (002) and (200) of the tetragonal phase. This splitting was observed in our $BaTiO_3$ particles as well (Figure 5). From the XRD of the tetragonal $BaTiO_3$, we found the c/a ratio to be 1.004. Although the particles became ferroelectric due to the high-temperature treatment, they lost sphericity and partially sintered together (Figure 5B).

Mixed perovskites have importance for tuning structural and dielectric properties. The phase diagram of $Ba_xSr_{1-x}TiO_3$ has cubic and tetragonal structures. In the case of the ternary perovskite $Ba_xSr_yCa_{1-x-y}TiO_3$, the orthorhombic phase also appears in the phase diagram.[15] To demonstrate that our method can equally well be used to prepare mixed perovskites, we have prepared $Ba_{0.5}Sr_{0.5}TiO_3$. The XRD pattern of the $Ba_{0.5}Sr_{0.5}TiO_3$ particles (Figure 6) showed peaks exactly between the corresponding peaks of $BaTiO_3$ and $SrTiO_3$. This means that the differently sized Ba and Sr atoms have mixed at a nanometer level causing the unit cell parameters to be averaged. We think that this nice averaging of the unit cell parameters is also evidence that the A/Ti ratio is close to unity, such that inside the colloidal particle metal salts disperse uniformly and that using two metal salts instead of one introduced no impurity peaks (for a full XRD pattern of the $Ba_{0.5}Sr_{0.5}TiO_3$ particles, see the Supporting Information, Figure S2).

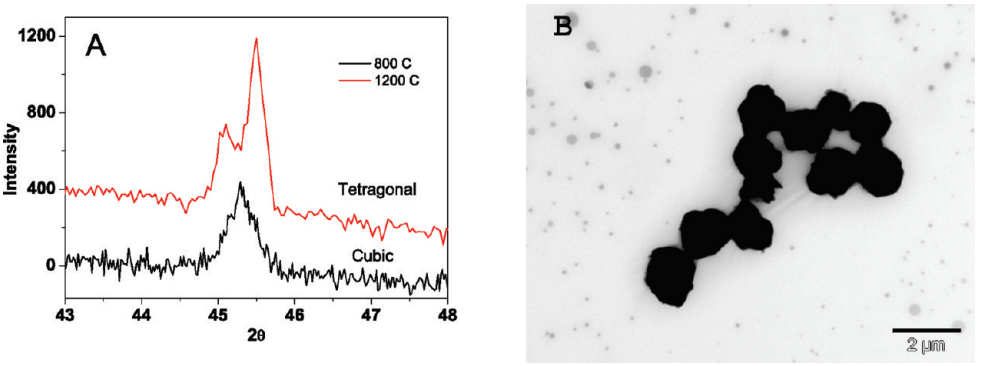

Figure 5. $BaTiO_3$ particles as synthesized are amorphous gels, but after calcination between 700 and 1000 °C, the particles are cubic in structure. Calcination at higher temperatures results in the tetragonal structure, which is known to be ferroelectric: (A) The change in structure from cubic to tetragonal causes a splitting of the (200) peak; (B) TEM image of $BaTiO_3$ particles calcined at 1200 °C for 1 h .

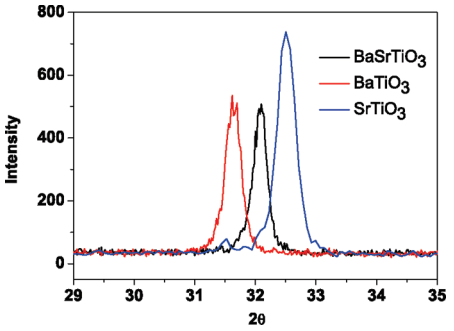

Figure 6. $Ba_{0.5}Sr_{0.5}TiO_3$ particles as synthesized are amorphous, but after calcination at 900 °C, we observe the mixed $Ba_{0.5}Sr_{0.5}TiO_3$ crystal structure with unit cell parameters averaged between those of $BaTiO_3$ and $SrTiO_3$. This averaging shows that the mixing is at atomic level and (Ba + Sr)/Ti ratio is close to unity.

To demonstrate the generality of our approach,we also fabricated Ag core−$BaTiO_3$ shell (Ag@$BaTiO_3$) particles starting from Ag@TiO_2 particles. Core−shell $BaTiO_3$ with a conductive core and with a ferroelectric shell is crucial for production of percolative capacitors.[12,18] The amorphous shell of Ag@$BaTiO_3$ crystallized upon calcination at 900 °C. It could be expected that silver oxide would have been formed due to contact with air, but this was not the case, as seen from the XRD pattern (see Supporting Information, Figure S3). We think that the oxidation is prohibited due to the thick layer of $BaTiO_3$. From the SEM image of the Ag@$BaTiO_3$ particles in Figure 7A, it was observed that the surface is similar in texture to the $BaTiO_3$ particle surface. The core−shell structure of the original particles can be seen in Figure 7B,C,D. Figure 7B is the TEM image of the Ag@TiO_2 particles, and Figure 7C,D is Ag@TiO_2 particles etched with concentrated HNO_3, partially and fully etched, respectively. Note that due to the softness of the shell, the fully etched particles in Figure 7D collapsed. From the SEM images, the Ag particles were estimated to be 250 ± 20 nm in size, whereas the Ag@TiO_2 particles were found to be 690 ± 45 nm from TEM image analysis (Supporting Information, Figure S4). The titania shell around the Ag core is therefore about 220 nm thick. The thickness affects the oxidation time for the oxidation of Ag, as well as the etching time of the Ag core with 65% (v/v) HNO_3. To our surprise, the Ag core of the Ag@TiO_2 particles was not yet fully etched after one night exposure to concentrated HNO_3, whereas bare Ag particles were etched in seconds under the same conditions. It was not possible to etch the Ag core in Ag@$BaTiO_3$ at all. Note that a similar result was found by Lee et al., although they only had a 10 nm thick $BaTiO_3$ shell.[12]

Our synthesis route offers the opportunity to easily manipulate the properties of the particles after the titania synthesis. To demonstrate this, we have successfully fabricated luminescent $Ca_{0.6}Sr_{0.4}TiO_3$ and $CaTiO_3$ particles doped with 0.2% Pr^{3+} salt by adding the salt into the dispersion of titania particles together with Ca or Ca, Sr mixed salts. The mixed dispersion was sonicated, dried, and calcined at 900 °C for 1 h. TEM images of Pr-doped perovskites and an XRD of the $Ca_{0.6}Sr_{0.4}TiO_3$ particles are shown in Figures S5 and S6 of Supporting Information. The luminescence peak at 613 nm of Pr:$CaTiO_3$ was clearly observed, and it was preserved in the $Ca_{0.6}Sr_{0.4}TiO_3$ case with a decrease in the intensity and shift to a lower wavelength, which is also known for bulk, see Figure 8.[15,31] As the Sr concentration increases the excitation intensity at 320 nm decreases, whereas the excitation intensity at 410 nm (broad) increases. For $Ca_xSr_{1-x}TiO_3$, it is also known that there is another emission at 491 nm that increases in intensity with an increase in the Sr ratio from $x = 0$ to $x = 0.3$.[15,32] The intensity of 491 nm emission has a maximum at $x = 0.3$, starts decreasing over 0.3 and vanishes at $x = 0.5$.[32] We also observed this emission of $Ca_{0.6}Sr_{0.4}TiO_3$ particles at 491 nm by only exciting with 410 nm wavelength but not with 320 nm (Figure S7, Supporting Information). Thus we think that the 410 nm excitation is the cause of the emission at 491 nm, which increases with the increase of Sr/Ti ratio. We have observed the luminescence of single particles under a microscope by exciting with a Hg lamp filtered for the 350−380 nm region. The red emission of the particles is clearly visible (Figure S8, Supporting Information).

4. Conclusion

We have reported an easy way of fabricating colloidal perovskite particles. Controlling access of metal salts to

(31) Diallo, P. T.; Boutinaud, P.; Mahiou, R.; Cousseins, J. C. *Phys. Status Solidi (a)* **1997**, *160*, 255.
(32) Jia, W.; Xu, W.; Rivera, I.; Perez, A.; Fernandez, F. *Solid State Commun.* **2003**, *126*, 153–157.

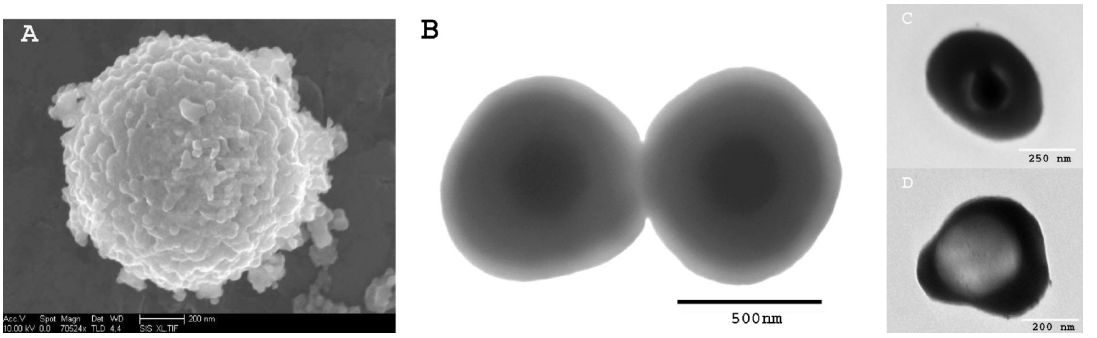

Figure 7. (A) An SEM image of $Ag@BaTiO_3$ particles after calcination with a rough surface, which indicates the shell to be $BaTiO_3$. (B) The original $Ag@TiO_2$ particles before $Ba(OH)_2$ treatment (contrast increased). $Ag@TiO_2$ particles (C) partially and (D) fully etched with concentrated HNO_3 for 1 and 2 days, respectively.

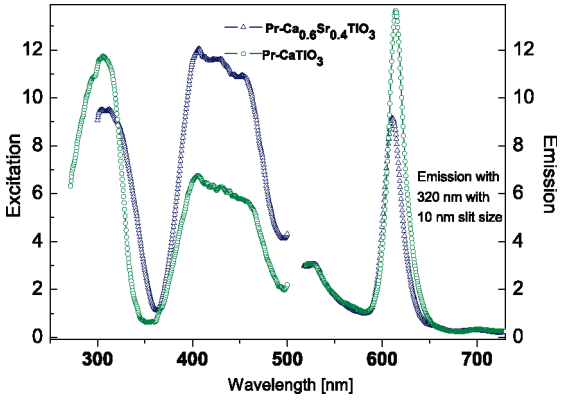

Figure 8. The excitation and emission spectra of Pr-doped $CaTiO_3$ and $CaSrTiO_3$ particles. Excitation spectra on the left were collected for the 613 nm emission, and the emission spectra on the right were excited with 320 nm with a 10 nm slit size in both cases.

the pores in the titania by an optional drying step shows that the synthesis relies on the porous structure of the as-synthesized titania particles. After calcination, the perovskites are highly crystalline and monodisperse in size. These colloidal particles are potentially important for making films for electronic and photonic applications. This method offers the flexibility of obtaining various types of perovskite structures simply by changing the metal salt. Various types of stable crystallographic structures can be made by mixing different kinds of metal salts, as shown in the example of $Ba_{0.5}Sr_{0.5}TiO_3$. The method also applies to core−shell particles as demonstrated for $Ag@BaTiO_3$. Additionally the method provides the flexibility of being able to play with the properties of the particles after the synthesis as in the example of doping the particles with Pr for luminescence.

Acknowledgment. The authors thank J.D. Meeldijk for the assistance with the EDX measurements, Stephane Badaire for SEM images and for synthesis of Ag particles, and Alfons van Blaaderen for fruitful discussions.

Note Added after ASAP Publication. This paper published ASAP May 14, 2008 with an error in the page number of the reference cited in the abstract; the corrected version published ASAP May 19, 2009.

Supporting Information Available: EDX spectra for perovskite particles, XRD of $Ba_{0.5}Sr_{0.5}TiO_3$ and $Ag@BaTiO_3$ particles, SEM image of Ag particles, TEM images of $CaTiO_3$ and $Ca_{0.6}Sr_{0.4}TiO_3$ particles, luminescence spectra for Pr-doped $Ca_{0.6}Sr_{0.4}TiO_3$ and microscopy images of Pr-doped perovskites (PDF). This material is available free of charge via the Internet at http://pubs.acs.org.